Available online at www.sciencedirect.com
SCIENCE DIRECT®
Journal of Solid State Chemistry 178 (2005) 1292–1300
JOURNAL OF SOLID STATE CHEMISTRY
www.elsevier.com/locate/jssc

Hydrogen-induced atomic rearrangement in $MgPd_3$

H. Kohlmann[a,b,*], G. Renaudin[a,c], K. Yvon[a], C. Wannek[d], B. Harbrecht[d]

[a]*Laboratoire de Cristallographie, Université de Genève, 24 Quai Ernest Ansermet, 1211 Genève 4, Switzerland*
[b]*Institut fur Anorganische und Analytische Chemie und Radiochemie, Universität des Saarlandes, 66041 Saarbrücken, Germany*
[c]*Laboratoire des Matériaux Inorganiques, Université Blaise Pascal de, Clermont-Ferrand, 24 avenue des Landais, 63177 Aubière Cedex, France*
[d]*Fachbereich Chemie, und Wissenschaftliches Zentrum für Materialwissenschaften Philipps-Universität Marburg, 35032 Marburg, Germany*

Received 21 December 2004; received in revised form 31 January 2005; accepted 1 February 2005

Abstract

The hydrogenation behavior of $MgPd_3$ has been studied by in situ X-ray powder diffraction and by neutron powder diffraction. At room temperature and $p \approx 500$ kPa hydrogen pressure its structure is capable of incorporating up to one hydrogen atom per formula unit (α-$MgPd_3H_{\approx 1}$), thereby retaining a tetragonal $ZrAl_3$-type metal atom arrangement. Upon heating to 750 K in a hydrogen atmosphere of 610 kPa it transforms into a cubic modification with $AuCu_3$-type metal atom arrangement (β-$MgPd_3H_{\approx 0.7}$). Neutron diffraction on the deuteride reveals an anion deficient anti-perovskite-type structure (β-$MgPd_3D_{0.67}$, $a = 398.200(7)$ pm) in which octahedral sites surrounded exclusively by palladium atoms are occupied by deuterium. Complete removal of hydrogen (480 K, 1 Pa) stabilizes a new binary modification (β-$MgPd_3$, $a = 391.78(2)$ pm) crystallizing with a primitive cubic $AuCu_3$-type structure. Mechanical treatment (grinding) transforms both α and β modifications of $MgPd_3$ into a cubic face-centered solid solution $Mg_{0.25}Pd_{0.75}$ showing a random distribution of magnesium and palladium atoms.

Keywords: Metal hydrides; Intermetallic compounds; Neutron diffraction; X-ray diffraction; Phase transition; Crystal structure determination

1. Introduction

Palladium and its intermetallic compounds have been extensively studied with respect to hydrogen sorption properties such as hydrogen embrittlement, order–disorder transitions, electronic and magnetic properties, lattice gas behavior of hydrogen, etc. [1,2]. A compound that has not yet been examined is the recently reported $MgPd_3$ [3], whose structure is closely related to that of cubic closest packed (ccp) palladium ($a = 389.16$ pm [4]). Complete ordering of the atoms at distinct sites is associated with a quadrupling of one of the cubic lattice vectors resulting in a superstructure with tetragonal lattice parameters $a = 392.26$ pm, $c = 1565.27$ pm [3] ($ZrAl_3$ type). In this work the structural changes of that compound during hydrogen absorption are studied in detail. It will be shown that depending on experimental conditions various structural modifications may occur. They differ mainly with respect to atomic order of the metal substructure, thus demonstrating the subtle influence of hydrogen on the structural stability of these types of compounds. Palladium–magnesium alloys are also of interest for the study of hydrogen-induced optical properties of magnesium containing thin films such as Mg_2Ni for which Pd is used as a capping layer in order to protect the samples from oxidation and promote hydrogen uptake [5,6].

2. Experimental section

2.1. Nomenclature

During the course of this work three different hydride phases $MgPd_3H_x$ ($x<1$) and three different $MgPd_3$

*Corresponding author. Institut für Anorganische und Analytische Chemie und Radiochemie, Universität des Saarlandes, Fachrichtung 8.1—Chemie, Postfach 151150, 66041 Saarbrücken, Germany. Fax: +49 681 302 4233.
E-mail address: h.kohlmann@mx.uni-saarland.de (H. Kohlmann).

0022-4596/$ - see front matter © 2005 Elsevier Inc. All rights reserved.
doi:10.1016/j.jssc.2005.02.001

phases were identified. For clarity, the following nomenclature will be used:

α-$MgPd_3$: ordered intermetallic compound, tetragonal $ZrAl_3$-type structure,
α-$MgPd_3H_x$: hydride based on α-$MgPd_3$, hydrogen-filled tetragonal $ZrAl_3$-type structure,
β-$MgPd_3$: ordered intermetallic compound, cubic $AuCu_3$-type structure,
β-$MgPd_3H_x$: hydride based on β-$MgPd_3$, hydrogen-filled cubic $AuCu_3$-type structure (anion deficient cubic anti-perovskite type),
$Mg_{0.25}Pd_{0.75}$: solid solution of magnesium in palladium, ccp with random distribution of magnesium and palladium,
$Mg_{0.25}Pd_{0.75}H_x$: hydride based on $Mg_{0.25}Pd_{0.75}$, hydrogen-filled ccp with disordered magnesium and palladium distribution.

2.2. Synthesis

$MgPd_3$ powder samples were synthesized as described earlier [3]. Hydrogenation (deuteration) experiments were carried out at moderately high hydrogen (deuterium) pressures and temperatures ($p(H_2) \leqslant 2$ MPa, $T \leqslant 750$ K) in steel autoclaves or in a reaction chamber mounted on an X-ray diffractometer (see Section 2.3). Hydrogenation at higher pressures (6.5 MPa) or with prolonged reaction times (several weeks) led to a deteriorated crystallinity as seen by ex situ X-ray analysis. The hydrogen contents of the hydride (deuteride) samples were determined gravimetrically and of the deuteride sample in addition by neutron diffraction. The samples were found to contain up to one hydrogen (deuterium) atom per formula unit. They released hydrogen almost completely if stored in open containers in air and could be dehydrogenated by mild heat treatment (480 K) in a vacuum (see last three entries in the last column of Table 1). Samples treated by the latter method showed no significant weight difference compared to the initial starting material and are therefore considered as hydrogen (deuterium) free within experimental error (≈ 0.05 H (D) atoms per formula unit). Samples for the neutron diffraction experiments were prepared by deuterating $MgPd_3$ in an autoclave at $T = 293$ and 750 K, $p(D_2) = 0.50$ and 1.6 MPa for 24 and 65 h for α and β phase deuterides, respectively. Gravimetrical analysis of the product right after opening the autoclave indicated a deuterium content of $MgPd_3D_{1.0(1)}$ for the β phase. Due to the above-mentioned hydrogen (deuterium) loss of samples at ambient conditions, however, the samples for neutron diffraction contained less than one deuterium per formula unit (see Sections 2.4, 3.2 and 3.3).

2.3. X-ray powder diffraction

Ex situ X-ray powder diffraction data were taken from flat samples with an internal silicon standard using a Guinier camera, a Bruker D8 Bragg-Brentano diffractometer or a Philips PW1820 Bragg-Brentano diffractometer (all CuK_α radiation). Samples placed in capillaries were investigated on a powder diffractometer installed at the European Synchrotron Radiation Facility in Grenoble, France (Swiss Norwegian Beam Line BM1, $\lambda = 49.949(1)$ pm for β-$MgPd_3$ and $\lambda = 85.022(1)$ pm for $Mg_{0.25}Pd_{0.75}$).

In situ X-ray powder diffraction experiments were performed in a PAAR reaction chamber as mounted on a Philips PW1820 diffractometer, diffraction angle range $10^\circ \leqslant 2\theta \leqslant 90^\circ$, step size $\Delta 2\theta = 0.025^\circ$, counting time 15 s/step). 2θ zero point shift and sample displacement were refined using the reflections of an internal silicon standard. Data were taken first on $MgPd_3$ in vacuum. In a second step the reaction chamber was filled with 500 kPa hydrogen (Carbagas, 99.999%) and diffraction data were collected at temperatures of 298, 360, 450, 550, 650 and 750 K, thereby increasing the hydrogen pressure to 610 kPa for the final temperature (Table 1). Further X-ray data were collected after cooling down to room temperature at various hydrogen pressures and after exposure to air for different lengths of time (Table 1). Data collection at each step started after the hydrogen pressure remained constant for a few hours, which insured that the hydrogen absorption or desorption reactions were finished.

2.4. Neutron powder diffraction

In order to prevent further deuterium desorption a β-$MgPd_3D_{0.67}$ sample was filled into a vanadium can (10 mm outer diameter, indium wire seal) immediately after opening the autoclave (see Section 2.2). Diffraction data were taken at the High Resolution Powder Diffractometer (HRPT) at the Paul-Scherrer Institut (Villigen, Switzerland) up to $2\theta = 165^\circ$ with a step size of $\Delta 2\theta = 0.05^\circ$ ($\lambda = 188.57$ pm). Under the same experimental conditions preliminary studies on a deuteride of α-$MgPd_3$ were carried out. All crystal structure refinements were carried out using the Rietveld method (program FullProf.98 [7]).

3. Crystal structure determination and refinement

3.1. Disordered cubic $Mg_{0.25}Pd_{0.75}$

Thorough grinding of α- and β-$MgPd_3$ in an agate mortar led to phase transformations. The superstructure reflections in the X-ray powder patterns of the new phase $Mg_{0.25}Pd_{0.75}$ had all vanished indicating a

Table 1
Unit cell dimensions of $MgPd_3$ and its hydrides as a function of hydrogen pressure and temperature as determined by in situ X-ray diffraction studies of the hydrogenation of α-$MgPd_3$ (containing small amounts of $Mg_{0.25}Pd_{0.75}$)

Compound	Metal atom substructure	Mole fraction α/β	T (K)	$p(H_2)$ (kPa)	a (pm)	c (pm)	V(f.u. $MgPd_3$) (10^6 pm^3)[a]	$\Delta V/V_0$[b] (%)
α-$MgPd_3$	$ZrAl_3$ type	100/0	298	0	392.60(3)	1561.6(2)	60.17(2) = V_0	0
$Mg_{0.25}Pd_{0.75}$	Cu type				391.65(2)		60.08(1)	−0.1
α-$MgPd_3H_x$	$ZrAl_3$ type	70/30	298	495	397.93(4)	1623.7(2)	64.28(2)	+6.8
β-$MgPd_3H_x$	$AuCu_3$ type				399.73(9)		63.87(4)	+6.1
$Mg_{0.25}Pd_{0.75}H_x$	Cu type				400.06(4)		64.03(2)	+6.4
α-$MgPd_3H_x$	$ZrAl_3$ type	53/47	360	500	397.97(5)	1607.8(3)	63.66(3)	+5.8
β-$MgPd_3H_x$	$AuCu_3$ type				399.53(5)		63.77(2)	+6.0
$Mg_{0.25}Pd_{0.75}H_x$	Cu type				399.34(2)		63.68(1)	+5.8
α-$MgPd_3H_x$	$ZrAl_3$ type	44/56	450	540	400.44(3)	1586.8(2)	63.61(2)	+5.7
β-$MgPd_3H_x$	$AuCu_3$ type				399.41(2)		63.72(1)	+5.9
$Mg_{0.25}Pd_{0.75}H_x$	Cu type				398.95(2)		63.50(1)	+5.5
α-$MgPd_3H_x$	$ZrAl_3$ type	34/66	550	570	400.53(3)	1583.8(2)	63.52(2)	+5.6
β-$MgPd_3H_x$	$AuCu_3$ type				399.80(1)		63.90(1)	+6.2
$Mg_{0.25}Pd_{0.75}H_x$	Cu type				398.37(2)		63.22(1)	+5.1
α-$MgPd_3H_x$	$ZrAl_3$ type	21/79	650	600	399.39(5)	1584.6(3)	63.19(3)	+5.0
β-$MgPd_3H_x$	$AuCu_3$ type				400.10(1)		64.05(1)	+6.4
$Mg_{0.25}Pd_{0.75}H_x$	Cu type				392.64(3)		60.53(1)	+0.6
β-$MgPd_3H_x$	$AuCu_3$ type	0/100	750	610	400.17(1)		64.08(1)	+6.5
$Mg_{0.25}Pd_{0.75}H_x$	Cu type				393.39(2)		60.88(1)	+1.2
β-$MgPd_3H_x$	$AuCu_3$ type	0/100	290	410	399.38(1)		63.70(1)	+5.9
$Mg_{0.25}Pd_{0.75}H_x$	Cu type				398.93(1)		63.49(1)	+5.5
β-$MgPd_3H_x$	$AuCu_3$ type	0/100	300	100	399.44(1)		63.73(1)	+5.9
$Mg_{0.25}Pd_{0.75}H_x$	Cu type				399.01(2)		63.53(1)	+5.6
β-$MgPd_3$ (after dehydrogenation at 480 K in vacuum)	$AuCu_3$ type	0/100	298	Air	391.78(2)		60.13(1)	−0.1
$Mg_{0.25}Pd_{0.75}$	Cu type				391.53(4)		60.02(2)	−0.2
β-$MgPd_3H_x$ (after 18 h in air)	$AuCu_3$ type	0/100	298	Air	395.71(7)		61.96(3)	+3.0
β-$MgPd_3$ (after 96 h in air)	$AuCu_3$ type	0/100	298	Air	391.88(2)		60.18(1)	0.0

[a] V(*f.u.* $MgPd_3$) = unit cell volume per formula unit $MgPd_3$. V_0 = cell volume of starting material per formula unit $MgPd_3$.
[b] Relative cell volume change $\Delta V/V_0 = (V - V_0)/V_0$. Note that the relative volume change $\Delta V/V_0$ represents the effects of both hydrogen incorporation and thermal expansion. The latter, however, is negligible as compared to the former.

complete loss of ordering (compare Figs. 1(a) and (f) with (b)) while the remaining reflections could be indexed to a face centered cubic cell. Reflection intensities were consistent with a cubic closest packed arrangement of atoms ($Fm\bar{3}m$, Mg/Pd in 4*a* 0, 0, 0, $a =$ 392.03(4) and 391.91(2) pm for samples prepared from α- and β-$MgPd_3$, respectively). Hence, this phase can be considered as a solid solution, which derives from the Cu-type palladium metal by substituting $\frac{1}{4}$ of the palladium by magnesium atoms in a random manner.

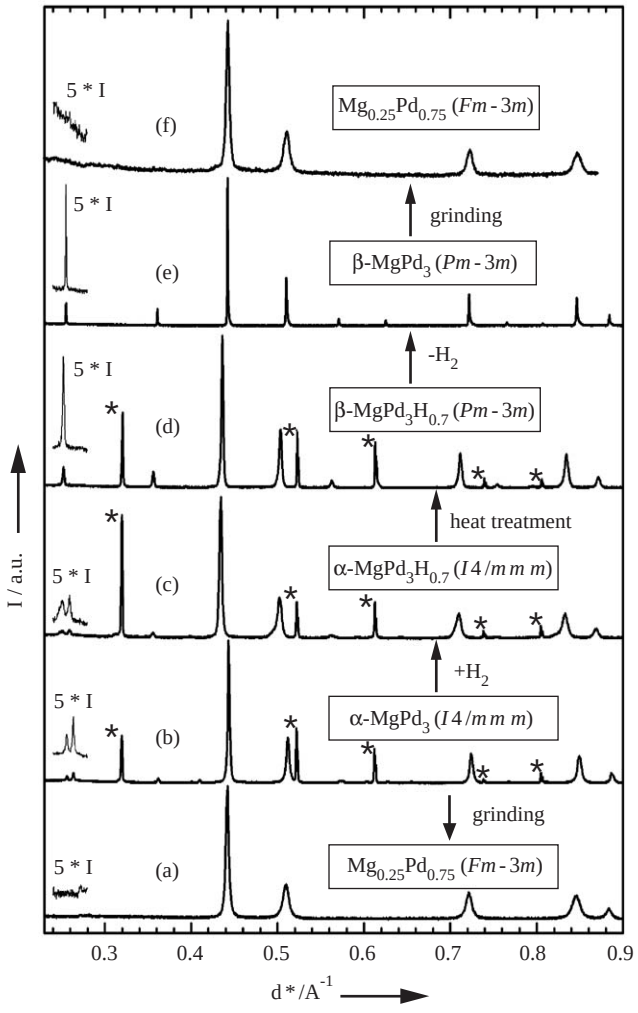

Fig. 1. X-ray powder diffraction study of hydrogenation-dehydrogenation and mechanical grinding of $MgPd_3$ (data at room temperature; renormalized to the same maximum intensity of the strongest reflection; silicon standard reflections marked with an asterisk (*); abscissa: $d^* = 1/d = 2\sin\theta/\lambda = Q/2\pi$). From bottom to top: (a) synchrotron powder diffraction pattern (SPD, $\lambda = 85.022(1)$ pm) of $Mg_{0.25}Pd_{0.75}$ synthesized by thorough grinding of α-$MgPd_3$, (b) X-ray powder diffraction pattern (XRPD) of α-$MgPd_3$, (c) XRPD of α-$MgPd_3H_{0.7}$ at $p(H_2) = 495$ kPa, (d) XRPD of β-$MgPd_3H_{0.7}$ at $p(H_2) = 100$ kPa (after heat treatment up to 750 K), (e) SPD ($\lambda = 49.949(1)$ pm) of β-$MgPd_3$ synthesized by dehydrogenation of β-$MgPd_3H_{0.7}$, (f) XRPD of a $Mg_{0.25}Pd_{0.75}$ sample synthesized by thorough grinding of β-$MgPd_3$. Inserts with five times the intensity show superstructure reflections (004) and (101) for (b) and (c), and (100) for (d) and (e). For details of sample treatment see text.

The composition for such a solid solution, prepared by thorough grinding of α-$MgPd_3$, was assured by means of EDX analyses (CamScan CS 4DV, Noran Instruments) resulting in 76(1) mol% Pd.

3.2. Ordered tetragonal α-$MgPd_3H_x$

In agreement with literature [3] α-$MgPd_3$ was found to adopt a tetragonal superstructure of a cubic closest packed arrangement ($ZrAl_3$ type, space group $I\,4/mmm$, Table 1). The compound takes up hydrogen to form a ternary hydride α-$MgPd_3H_x$ and small amounts of cubic primitive β-$MgPd_3H_x$ (see Section 3.3). α-$MgPd_3$ undergoes a considerable lattice expansion upon hydrogenation (see Table 1), but retains its $ZrAl_3$-type metal atom arrangement. Note the shift in reflection positions upon hydrogen uptake (compare Fig. 1(b) and (c)). Preliminary neutron diffraction studies on a deuterated sample, which, however, was found to be a mixture of deuterium-free α-$MgPd_3$ and α-$MgPd_3D_{0.42(1)}$ ($a = 395.67(1)$ pm, $c = 1571.18(7)$ pm) showed deuterium occupation of octahedral interstices exclusively surrounded by six palladium atoms ([Pd_6]).

3.3. Ordered cubic β-$MgPd_3H_x$

After hydrogenation the $MgPd_3$ samples not only contain the α-$MgPd_3H_x$ phase but also small amounts of a further hydride phase, β-$MgPd_3H_x$. The conversion from α- to β-$MgPd_3H_x$ proceeds with increasing temperature and is complete at 750 K (Table 1). X-ray reflections of β-$MgPd_3H_x$ could be indexed to a primitive cubic unit cell and intensities were consistent with a $AuCu_3$-type metal atom arrangement. In order to determine the hydrogen positions neutron diffraction

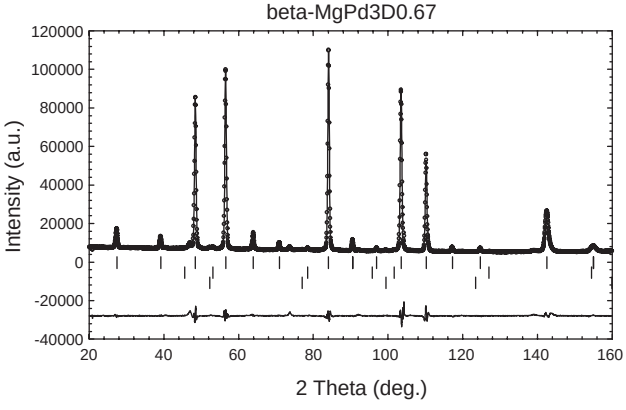

Fig. 2. Rietveld refinement of the crystal structure of β-$MgPd_3D_{0.67}$ on neutron powder diffraction data (HRPT, Paul-Scherrer Institut, Villigen, Switzerland; $\lambda = 188.57$ pm). Observed (circles), calculated (solid line) and difference (observed—calculated; bottom) neutron powder diffraction patterns of β-$MgPd_3D_{0.67}$. Markers indicate Bragg peak positions of (from top to bottom) β-$MgPd_3D_{0.67}$, MgO (traces) and V (sample container).

Table 2
Crystal structure of β-$MgPd_3D_{0.67}$ as refined from neutron powder diffraction data at room temperature and interatomic distances in pm below 350 pm, space group $Pm\bar{3}m$ (No. 221), $a = 398.200(7)$ pm

Atom	Site	x	y	z	B_{iso} (10^4 pm^2)	Occupation
Mg	1*a*	0	0	0	0.78(3)	1
Pd	3*c*	0	$\frac{1}{2}$	$\frac{1}{2}$	0.69(2)	1
D	1*b*	$\frac{1}{2}$	$\frac{1}{2}$	$\frac{1}{2}$	2.20(5)	0.668(4)
$R_p = 0.028$, $R_{wp} = 0.046$, $R'_p = 0.109$, $R'_{wp} = 0.106$, $R_{Bragg} = 0.029$						
Pd–2D	199.10(1)	Mg–8D	344.85(1)	D–6Pd	199.10(1)	
Pd–4Mg	281.57(1)	Mg–12Pd	281.57(1)	D–8Mg	344.85(1)	
Pd–8Pd	281.57(1)					

Definition of R factors: $R_p = \Sigma|y_i(\text{obs})-y_i(\text{calc})|/\Sigma y_i(\text{obs})$; $R_{wp} = [\Sigma w_i(y_i(\text{obs})-y_i(\text{calc}))^2/\Sigma w_i y_i(\text{obs})^2]^{1/2}$; R'_p and R'_{wp} are calculated as above but using background corrected counts; $R_{Bragg} = \Sigma|I_B(\text{'obs'})-I_B(\text{calc})|/\Sigma I_B(\text{'obs'})$. Form of the temperature factor: $\exp[-B_{iso}(\sin\theta/\lambda)^2]$.

experiments were carried out on a deuterated sample whose X-ray diffraction pattern showed a single cubic primitive phase with $a = 398.34(5)$ pm. The neutron patterns revealed traces of MgO not seen in the X-ray patterns and some weak reflections of the container material vanadium (Fig. 2). The $AuCu_3$-type metal atom arrangement was confirmed and deuterium was found to occupy only those octahedral interstices which are surrounded by six palladium atoms (occupancy 66.8(4)%), i.e. the structure can be considered as a defect variant of the cubic anti-perovskite type (Table 2, Fig. 3). The structure refinement included 16 free parameters in the final cycles: one zero point correction in 2θ, one scale factor and one lattice parameter each for β-$MgPd_3D_{0.67}$, MgO and V, three halfwidth, one mixing (pseudo-Voigt profile function) and one asymmetry parameter, which were constrained to be the same for all three phases, three thermal displacement and one occupational factor for deuterium in β-$MgPd_3D_{0.67}$. Small additional reflections at 47.0° and 73.7° in 2θ could not be accounted for. A graphical representation of the Rietveld refinement results is shown in Fig. 2.

4. Discussion

4.1. Phase transitions in $MgPd_3$ induced by hydrogenation and mechanical treatment

Hydrogenation of α-$MgPd_3$ (Fig. 1b) at room temperature yields the hydride α-$MgPd_3H_x$ with an unchanged but expanded tetragonal $ZrAl_3$-type metal atom arrangement (6.8% cell volume expansion at 495 kPa hydrogen pressure, Fig. 1c, Table 1) and small amounts of cubic primitive β-$MgPd_3H_x$. During heating the former (α) loses hydrogen (see decrease of cell volume in Table 1) and converts into the latter (β), which shows fairly constant hydrogen content. At 750 K the transformation is complete (Table 1) and the formed β-$MgPd_3H_x$ retains hydrogen as long as it is stored in a hydrogen atmosphere (Fig. 1d). When stored in air, however, the compound loses hydrogen. Complete removal of hydrogen can be accomplished by gentle heating (480 K) in vacuum, producing a hitherto unknown second modification of intermetallic $MgPd_3$ (β) crystallizing in a $AuCu_3$-type structure (Fig. 1e, Table 1). The observed hydrogenation reactions

$$\alpha\text{-}MgPd_3 \leftrightarrow \alpha\text{-}MgPd_3H_x \quad \text{and} \quad \beta\text{-}MgPd_3 \leftrightarrow \beta\text{-}MgPd_3H_x$$

are completely reversible, in contrast to the $\alpha \rightarrow \beta$ transition for the hydrides which—by all indications—is irreversible. No such $\alpha \rightarrow \beta$ transition for the intermetallic compounds has been found in the absence of hydrogen even after prolonged annealing at high temperatures.

Upon heavy grinding in an agate mortar $MgPd_3$ (both α and β) transforms to a cubic solid solution $Mg_{0.25}Pd_{0.75}$ (Fig. 1(a) and (f)). This modification was often present in small amounts even in only gently ground α-$MgPd_3$ samples as indicated by an apparent splitting of X-ray reflections at high diffraction angles. It shows a reversible hydrogen uptake at room temperature similar to that of α-$MgPd_3$, but a more pronounced hydrogen loss upon heating. According to the Mg–Pd phase diagram in Ref. [8] a solid solution of composition $Mg_{0.25}Pd_{0.75}$ is thermodynamically stable only at high temperatures (1550 K), and at room temperature the maximum solubility of magnesium in palladium is reported to be 18% [8], in contrast to the value of 25% reported previously in Ref. [9]. Irrespective of this conflicting data we conclude on the basis of our preparative findings that the ordered α phase is the thermodynamically stable one at ambient temperature and that the formation of the ccp solid solution $Mg_{0.25}Pd_{0.75}$ at ambient conditions is triggered by tribochemical activation during grinding. The observed X-ray reflection broadening in $Mg_{0.25}Pd_{0.75}$ (compare Figs. 1(a) and (f) to (b)–(e)) suggests considerable internal stress in the material. The unit cell volumes per formula unit for the three different $MgPd_3$ phases are very similar ($Mg_{0.25}Pd_{0.75}$: 60.25(1), α-$MgPd_3$: 60.17(1), β-$MgPd_3$: 60.13(1)*10^6 pm^3). This indicates

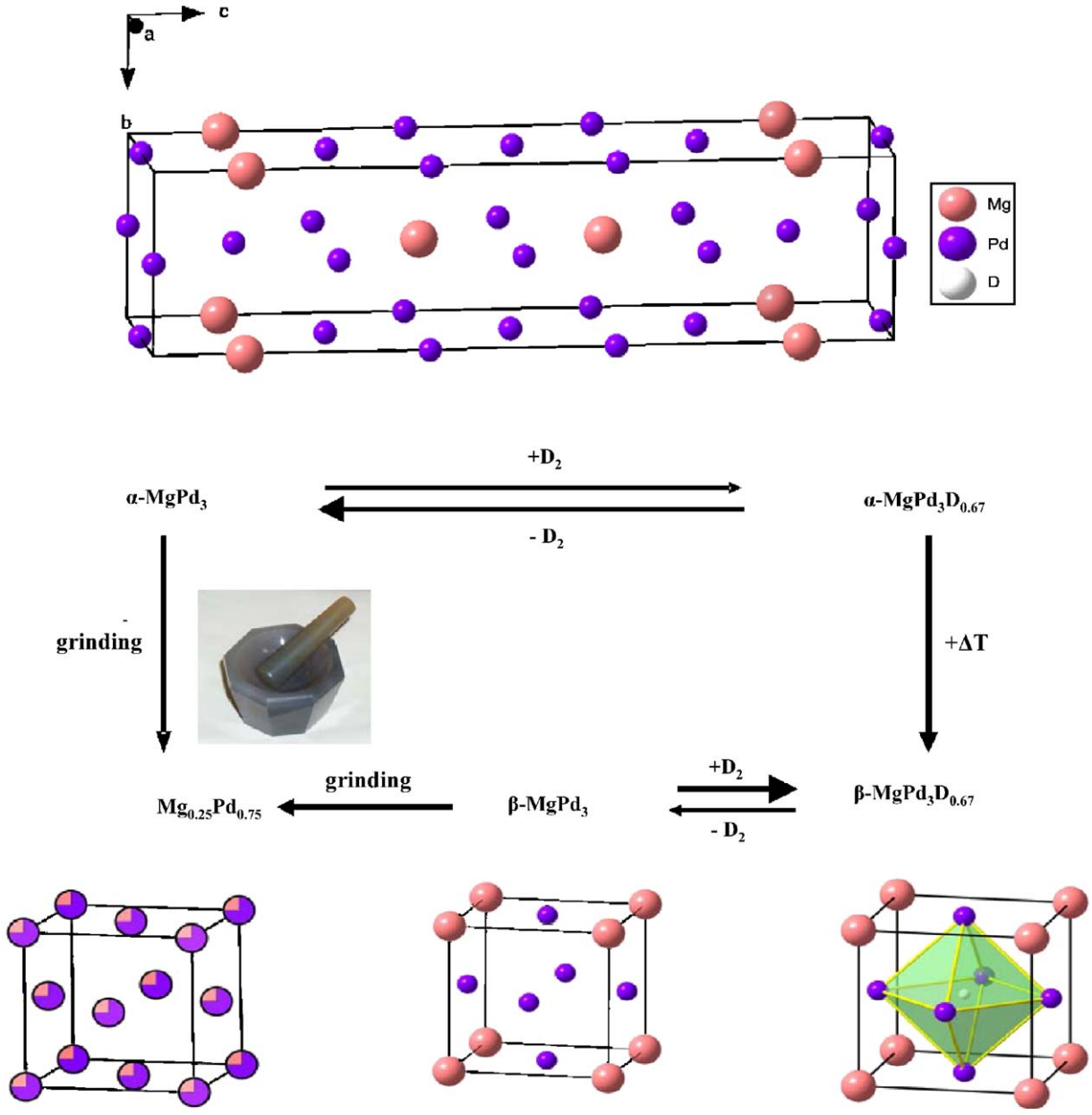

Fig. 3. Crystal structures of two ordered and one disordered modification of $MgPd_3$ and the deuteride β-$MgPd_3D_{0.67}$: α-$MgPd_3$ (after Ref. [3], β-$MgPd_3D_{0.67}$ (by neutron diffraction), β-$MgPd_3$ (by synchrotron diffraction) and $Mg_{0.25}Pd_{0.75}$ (by synchrotron diffraction). Deuterium positions in β-$MgPd_3D_{0.67}$ have been established by neutron diffraction and show occupancy of 66.8(4)%. Note that the deuteration–dedeuteration cycle from α-$MgPd_3$ to β-$MgPd_3$ indicated in the drawing corresponds to the hydrogenation-dehydrogenation shown in Fig. 1.

that the solid solution formed by grinding indeed has a stoichiometry close to 1:3, which is also supported by EDX measurements (see Section 3.1), and that, by all indications, β-$MgPd_3$ obtained by dehydrogenation of its hydride is hydrogen free.

4.2. Crystal chemistry of $MgPd_3$ hydrides

Hydrogen induces an atomic rearrangement from one type of ccp superstructure ($ZrAl_3$ type in ordered tetragonal α-$MgPd_3H_x$) to another ccp superstructure ($AuCu_3$ type in ordered cubic β-$MgPd_3H_x$). Deuterium was found to partially occupy octahedral interstices surrounded exclusively by palladium atoms ([Pd_6]) both in α-$MgPd_3D_{0.42}$ and β-$MgPd_3D_{0.67}$. Octahedral sites with other surroundings, such as [$MgPd_5$] and [Mg_2Pd_4] are empty. Hydrogen (deuterium) is thus incorporated in the same local environment [Pd_6] as in $PdH_{\approx 0.7}$ with nearly the same occupation factor (β phase) and Pd–D distances (198 pm (α), 199 pm (β), as compared to

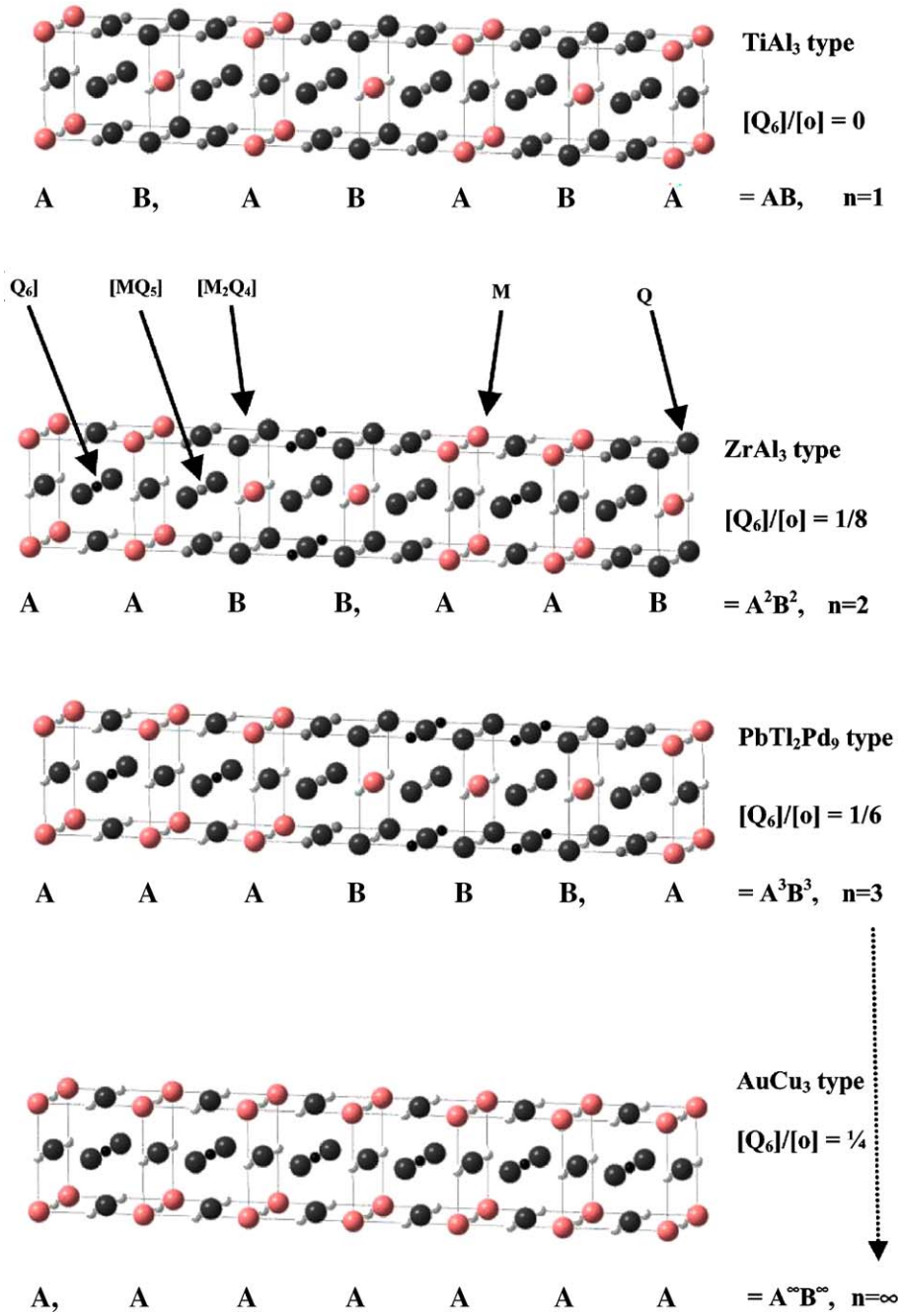

Fig. 4. Octahedral voids in intermetallic superstructures MQ_3 of the $AuCu_3$ type built up by stacking of n atomic MQ_3 double layers A and B, both shifted by $\frac{1}{2}\mathbf{a}+\frac{1}{2}\mathbf{b}$ with respect to each other (see text). Three different types of voids exist, $[M_2Q_4]$ (small white spheres), $[MQ_5]$ (small grey spheres) and $[Q_6]$ (small black spheres). The nomenclature indicates the number of M (large grey spheres, pink in color print) and Q atoms (large black spheres) surrounding these interstices and [o] denotes the sum of all octahedral voids.

201 pm in β-$PdD_{0.67}$ [10]). Only two other structure types are known for ternary palladium hydrides with divalent metals. A_2PdH_4 (A = Sr, Ba, Eu) adopts the β-K_2SO_4-type structure and contains 18-electron hydrido complexes $[PdH_4]^{4-}$, $APdH_{3-x}$ (A = Ca ($x = 1$), Sr ($x = 0.3$), Eu ($x = 0$)) crystallize in the cubic perovskite type and are probably metallic [11–14]. β-$MgPd_3H_{0.67}$ is the first magnesium palladium hydride fully structurally characterized. Its cubic anti-perovskite like structure is also well known to be adapted by numerous ternary metal borides, carbides, (sub)nitrides, and oxides. Hence, β-$MgPd_3H_{0.67}$ shows parallels to other typical interstitial and substoichiometric compounds. The hydrogen-induced rearrangement found in $MgPd_3$ resembles that in $MnPd_3$, which also reorders from a $ZrAl_3$-type to a $AuCu_3$-like structure [15–17]. The

difference in free energies for α and β modifications was found to be negligible in the latter system, both for the intermetallic compounds and the corresponding hydrides [18]. It was thus proposed that the observed $\alpha \rightarrow \beta$ transition in $MnPd_3$ upon hydrogenation is due to kinetic effects, such as stress-assisted atomic displacements around hydrogen occupied interstices in the α phase [18]. Here we suggest an alternative explanation, based on crystal-chemical reasoning, for the force driving the $\alpha \rightarrow \beta$ transition in $MnPd_3$ and $MgPd_3$.

The $ZrAl_3$ type of $MgPd_3$ is a member of a series of superstructures of the $AuCu_3$ type formed by the introduction of anti-phase boundaries $\frac{1}{2}$ [110] (Fig. 4) [3]. If such anti-phase boundaries occur after every atomic double-layer MQ_3 the stacking sequence is AB ($TiAl_3$ type, $n = 1$), if they occur after every other double-layer it is $AABB$ ($ZrAl_3$ type, $n = 2$), etc. ($PbTl_2Pd_9$ type, $n = 3,\ldots$, $AuCu_3$ type, $n = \infty$; Fig. 4). The stacking sequence determines which types of octahedral interstices are found in the various MQ_3 structures. $[Q_6]$-type voids can only occur between double-layers of the same kind, i.e. at interfaces AA or BB. Therefore, $[Q_6]$ can be easily enumerated as $2(n-1)$. As per anti-phase boundary the number of cubic subcells is doubled, each of which contains four octahedral holes, the total number of octahedral interstices [o] for a given superstructure is $8n$. The fraction of $[Q_6]$ of the total number of all octahedral voids [o] is therefore calculated as $[Q_6]/[o] = \frac{1}{4}(n-1)\,n^{-1}$, which converges for $n \rightarrow \infty$ to a maximum value of $\frac{1}{4}(A^{\infty}B^{\infty})$. Thus, the $AuCu_3$ type has the largest number of $[Q_6]$ for all possible superstructures ($1 \leqslant n \leqslant \infty$) formed by introducing anti-phase boundaries $\frac{1}{2}$ [110].

In view of the observed preference of hydrogen for $[Pd_6]$-type voids in a $MgPd_3$ intermetallic matrix (Fig. 3, Table 2), the $AuCu_3$-type is clearly favored over the $ZrAl_3$ type and all other superstructures. The increase of the configurational entropy by maximizing the number of $[Pd_6]$ interstices might be a driving force for the $\alpha \rightarrow \beta$ transition in $MgPd_3H_x$. Electronic factors may also play an important role, since high valence electron concentrations (VEC) were found to favor the $ZrAl_3$ type over the $AuCu_3$ in intermetallic compounds [19]. Assuming hydrogen to be an electron acceptor, the lowering of the VEC upon hydrogenation will thus favor the $AuCu_3$ type (β-$MgPd_3H_x$) over the $ZrAl_3$-type structure (α-$MgPd_3H_x$).

5. Conclusion

Atomic rearrangements in $MgPd_3$ may be introduced either by hydrogenation at 750 K or by mechanical treatment. Hydrogenation of $ZrAl_3$-type α-$MgPd_3$ leads first to a hydrogen incorporation in the intermetallic structure (α-$MgPd_3H_x$) at moderate pressures (<1 MPa), followed by a reordering of the metal lattice into a $AuCu_3$-type arrangement upon heating to 750 K. Hydrogen in the latter hydride β-$MgPd_3H_x$ is found to occupy exclusively octahedral sites surrounded by palladium only, resulting in a cubic anti-perovskite like structure. This strong preference of $[Pd_6]$ interstices for hydrogen occupancy might be the driving force for the transformation from α-$MgPd_3H_x$ to β-$MgPd_3H_x$, since their number is doubled in the latter with respect to the former. Hydrogen can be removed from this hydride to yield in the new intermetallic phase β-$MgPd_3$, which crystallizes in a cubic $AuCu_3$-type structure. Thus, tetragonal α-$MgPd_3$ may be converted to cubic β-$MgPd_3$ by a hydrogenation-dehydrogenation cycle. This transition does not proceed by heat treatment in the absence of hydrogen. Another transformation occurs in $MgPd_3$ (both α and β) upon mechanical treatment (grinding), which produces $Mg_{0.25}Pd_{0.75}$ with a cubic closest packing and statistical distribution of magnesium and palladium. The rearrangements found in $MgPd_3$ demonstrate the subtle influence of hydrogen on atomic order and stability in such intermetallic compounds.

Acknowledgments

We thank T. Hermannsdörfer (PSI) and Yaroslav Filinchuk (University of Geneva) for help with the neutron diffraction measurement and the team at SNBL for their support with the synchrotron diffraction experiment. This work has been supported by the Swiss Federal Office of Energy, the Swiss National Science Foundation and the German Research Foundation (DFG).

References

[1] T.B. Flanagan, Y. Sakamoto, Platinum Met. Rev. 37 (1993) 26–37.
[2] H. Kohlmann, Metal hydrides, in: R.A. Meyers (Ed.), Encyclopedia of Physical Sciences and Technology, vol. 9, Academic Press, New York, 2002, pp. 441–458.
[3] C. Wannek, B. Harbrecht, J. Solid State Chem. 159 (2001) 113–120.
[4] I.S. Balbaa, P.A. Hardy, A. San-Martin, P.G. Coulter, F.D. Manchester, J. Phys. F: Met. Phys. 17 (1987) 2041–2048.
[5] T.J. Richardson, J.L. Slack, R.D. Armitage, R. Kostecki, B. Farangis, M.D. Rubin, Appl. Phys. Lett. 78 (2001) 3047–3049.
[6] S. Enache, W. Lohstroh, R. Griessen, Phys. Rev. B: Condens. Matter 69 (2004) 115326.
[7] J. Rodriguez-Carvajal, Full Prof.98, 1998 (LLB, unpublished).
[8] A.A. Nayeb-Hashemi, J.B. Clark, Bull. Alloy Phase Diagrams 6 (1985) 164.
[9] R. Ferro, J. Less-Common Met. 1 (1959) 424–438.
[10] J.E. Schriber, B. Morosin, Phys. Rev. B: Condens. Matter 12 (1975) 117–118.
[11] W. Bronger, K. Jansen, P. Müller, J. Less-Common Met. 161 (1990) 299–302.

[12] W. Bronger, G. Ridder, J. Alloy Compd. 210 (1994) 53–55.
[13] M. Olofsson-Martenson, M. Kritikos, D. Noreus, J. Am. Chem. Soc. 121 (1999) 10908–10912.
[14] H. Kohlmann, H.E. Fischer, K. Yvon, Inorg. Chem. 40 (2001) 2608–2613.
[15] P. Önnerud, Y. Andersson, R. Tellgren, P. Norblad, F. Bourée, G. André, Solid State Commun. 101 (1997) 433–437.
[16] P.-J. Ahlzén, Y. Andersson, R. Tellgren, D. Rodic, Z. Phys. Chem. Neue Folge 163 (1989) 213–218.
[17] R. Tellgren, Y. Andersson, I. Goncharenko, G. André, F. Bourée, I. Mirebeau, J. Solid State Chem. 161 (2001) 93–96.
[18] P. Kumar, M. Hareesh, R. Balasubramaniam, J. Alloy Compd. 217 (1995) 151–156.
[19] A. Raman, K. Schubert, Z. Metallkde. 56 (1965) 99–104.